Available online at www.sciencedirect.com
ScienceDirect
Superlattices and Microstructures 40 (2006) 513–518
Superlattices and Microstructures
www.elsevier.com/locate/superlattices

Photoluminescence, cathodoluminescence, and reflectance study of AlN layers and AlN single crystals

G.M. Prinz[a,*], A. Ladenburger[a], M. Feneberg[a], M. Schirra[a], S.B. Thapa[b], M. Bickermann[c], B.M. Epelbaum[c], F. Scholz[b], K. Thonke[a], R. Sauer[a]

[a] *Institut für Halbleiterphysik, Universität Ulm, D-89069 Ulm, Germany*
[b] *Institut für Optoelektronik, Universität Ulm, D-89069 Ulm, Germany*
[c] *Institut für Werkstoffwissenschaften 6, Universität Erlangen, D-91058 Erlangen, Germany*

Received 25 September 2006; accepted 6 October 2006
Available online 22 November 2006

Abstract

Strained AlN layers grown by MOVPE on sapphire and nominally unstrained AlN single crystals were studied employing photoluminescence, cathodoluminescence, and reflectance spectroscopy in the near-band edge range. The data allow one to determine fundamental optical parameters such as the band edge energy with its crystal field splitting and strain dependence which are still under discussion. Reflection measurements performed on crystal facets with different orientations and subjected to varying selection rules serve to assign the observed transitions to valence band states with specific symmetries.

Near-band edge excitonic luminescence at around 6 eV was recorded as a function of temperature (8 . . . 300 K). Fits to the data using standard models from the literature yield the temperature dependence $E_g(T)$ of the band gap.

Keywords: Aluminium nitride; Cathodoluminescence; Photoluminescence; Reflectance spectroscopy

1. Introduction and experimental

Aluminium nitride (AlN) has a very wide band gap of approximately 6.1 eV at low temperature marking the "upper end" of the ternary AlGaN alloy system and making it an interesting material for optoelectronic applications in the deep UV region. Recent reports on

* Corresponding author. Tel.: +49 731 50 26127; fax: +49 731 50 26108.
E-mail address: Guenther.Prinz@uni-ulm.de (G.M. Prinz).

0749-6036/$ - see front matter © 2006 Elsevier Ltd. All rights reserved.
doi:10.1016/j.spmi.2006.10.001

successful Si doping with promising electron mobilities [1,2] suggest possible applications also for electronic devices in the high power–high temperature regime.

Despite numerous publications in the past years on the optical properties of AlN, there are still ongoing discussions on the assignment of a number of peaks observed in cathodoluminescence (CL) or photoluminescence (PL) measurements close to the band edge. Recent optical investigations of AlN single crystals and layers on various substrates [3–5] suggest a model of the band structure, in which the A valence band is separated by approximately 0.2 eV from the B and C valence bands, which in turn are split by an energy of order 10 meV only.

In the present work different nominally unstrained AlN single crystals with *c*-, *r*-, and *m*-plane facets and AlN layers grown on sapphire were studied. Temperature dependent CL, PL, and optical reflection measurements under different angles of incidence taken on the same samples allow a reliable assignment of the observed peaks to free and bound exciton transitions.

The AlN single crystals used here were grown in a tungsten crucible at temperatures of approximately 2250 °C and pressures below 1000 mbar. The crystals grew self-nucleated at the colder walls of the crucible up to a size of $10 \times 5 \times 3$ mm^3. Further details can be found in references [6,7]. The nominally 550 nm thick undoped AlN layers were grown in an Aixtron AIX 200 RF LP-MOVPE system on slightly off-axis oriented *c*-plane sapphire substrates using the standard precursors TMAl and ammonia on a thin AlN nucleation layer deposited at 900 °C and 100 mbar. The AlN layers were grown at 1150 °C and 35 mbar. The carrier gas consisted mainly of N_2 and H_2 in a 3:1 mixture with a total flow of 2300 sccm. The V-III ratio was 1000 and 600 for the samples Y968 and Y973, respectively, with low flow rates of both, ammonia and TMAl.

For the CL measurements a continuous flow cryostat allowed a choice of temperature from ≈10 K to room temperature (RT). The electron beam originated from a RHEED electron gun operated mostly at 6 kV acceleration voltage. A continuous flow cryostat similar to that for CL was used for the PL measurements, and the excitation source was a pulsed ArF excimer laser. The reflection measurements were carried out in the same cryostat as for the PL measurements, using a deuterium lamp as light source. In all experiments, the light was dispersed by a monochromator with a focal length of 1 m using a 1200 grooves/mm grating, and detected by a UV-optimized LN_2-cooled CCD camera. The whole light path was flushed with N_2 gas. The reflectance was measured in two different configurations, either at perpendicular incidence to the sample surface or at 45° incidence angle. These measurements were carried out at about 10 K. The spectra were corrected for the wavelength dependent sensitivity of the setup.

2. Results and discussion

The low temperature reflection measurements taken under different angles of incidence are compared to the corresponding CL or PL spectra in Figs. 1 and 2. The reflection spectra for both AlN layers (Fig. 1(a)+(b)) show strong Fabry–Pérot oscillations, the period of which allows to calculate a layer thickness of ≈570 nm for both samples. The Fabry–Pérot oscillations vanish at around 6.2 eV, indicating the onset of absorption. At ≈6.25 eV, we observe a broad resonance in all spectra and assign it – in accordance with other groups [3,4] – to an unresolved superposition of the X_B and X_C free exciton transitions, which are broadened by strong damping. This is consistent with the prediction that the energetic spacing of the two exciton lines is only around 14 meV. When the spin–orbit splitting is much smaller than the crystal field splitting, only the X_B and X_C exciton features can be observed under perpendicular incidence of light according to the selection rules [3] (Fig. 1(a)+(b), upper traces). For inclined incidence (lower traces in Fig. 1(a)+(b)) also the X_A transition is expected to appear, since for electric field vector

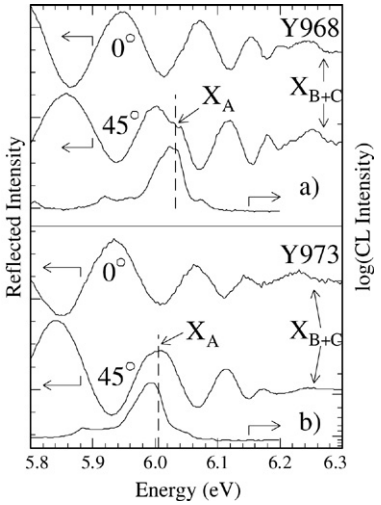

Fig. 1. Upper curves on the (a) and (b) panels: Reflectance measurements for the AlN layers Y968 and Y973 on *c*-plane sapphire. The curves are dominated by Fabry–Pérot oscillations. Lower curve on the two panels: Corresponding CL measurements.

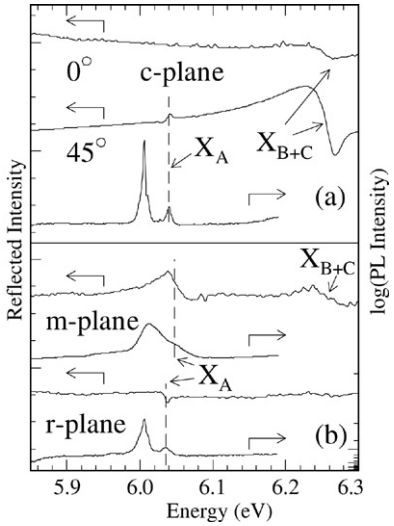

Fig. 2. (a) Upper two curves: Reflectance measurements for the *c*-plane of an AlN single crystal. Lower curve: Corresponding PL measurement. (b) Upper two curves: Reflectance and PL measurement on *m*-plane sample. Lower two curves: Reflectance and PL measurement on *r*-plane sample.

$\vec{E} \parallel \vec{c}$ a large oscillator strength of X_A is calculated. Indeed, an additional structure is observed at ≈6.0 . . . 6.04 eV dependent on the sample, which we assign to the X_A free exciton transition. This observation corroborates the assumption that the spin–orbit splitting is small compared to the crystal field splitting.

The lower curves in Fig. 1(a)+(b) are CL spectra for the two MOVPE layers, and Fig. 2(a) shows the PL spectrum of the *c*-plane single crystal. These spectra were all taken at 10 K. The single crystal exhibits two sharp lines (≈6.01 and 6.04 eV), whereas only a broad hump emerges

for the two MOVPE layers. Lineshape fits to the broad hump suggest three underlying line components. In accordance with the reflection measurements discussed above and the temperature dependent CL measurements (see below), we assign the highest-energy component to the X_A free exciton recombination. In all samples, several types of donor bound excitons (D^0, X) seem to be present: A shallow bound exciton with localization energy of $E_{\mathrm{loc,DX}} \approx 11 \ldots 13$ meV, and a few deeper bound excitons with $E_{\mathrm{loc,DX}} \approx 23 \ldots 35$ meV. One of the deeper binding impurities might be associated with silicon donors [2]. In most samples we observe a higher energy line typically ≈40 meV above the X_A peak. It disappears at intermediate temperatures together with the shallow (D^0, X) line and therefore, may originate from an excited state of the donor bound exciton.

The position of the X_A free exciton transition varies from sample to sample, unexpectedly even for the single crystal specimens: For the *c*-plane facet single crystal we find a value of 6.040 eV, for the *r*-plane sample 6.036 eV, and for the *m*-plane sample ≈6.05 eV. We assume that the shifts are due to different concentrations of impurities and defects causing a (small) change in the lattice constant. Thus, even for the unstrained bulk samples, it is not possible to quote an "ideal" excitonic band gap energy. For the AlN layers grown on sapphire we obtain X_A line positions of 6.033 eV (Y968) and 6.001 eV (Y973). Here, the diverse values are an indication of different strain governed by dissimilarities of the thermal expansion coefficients of the layer and the substrate, and different nucleation conditions. In Fig. 2(b) we show for comparison also the PL and reflection spectra for the *r*-plane and *m*-plane single crystals. The reflection spectra were taken under perpendicular incidence and show less pronounced features presumably due to the existing higher surface roughness. For both samples we find a clear resonance at ≈6.04 eV which we assign to the X_A exciton. The combined $X_B + X_C$ resonance at ≈6.25 eV seems to be more damped in these samples. The lower spectra on the two panels of Fig. 2 show the corresponding PL measurements for both samples. In the case of the *r*-plane single crystal, we observe two narrow lines, of which we assign the higher energy line to the X_A free exciton recombination. For the *m*-plane sample the lines are very broad, and we observe the X_A free exciton transition only as a shoulder on the main peak centered at ≈6.0 eV. To distinguish between free and bound exciton lines, we performed temperature-dependent CL or PL measurements on all samples. Two examples are shown in Fig. 3 depicting a series of CL spectra from the MOVPE AlN layer (Y968) at varied temperatures (8…300 K), and a series of PL spectra recorded from the *r*-plane single crystal. In both series we observe a take-over of the intensities from the donor bound excitons dominating at low temperatures to the X_A free exciton transition dominating the spectra at higher temperatures.

Fig. 4 shows the temperature dependence of the X_A and D^0X line positions for an AlN layer (Y968) and the *r*-plane single crystal. For both samples we fitted the data points using the Varshni [8], Viña [9], and Pässler [10] models. Whereas the phenomenological Varshni model yields only poor agreement, the Viña model fits the data much better. The best fits could be made employing the Pässler model describing the temperature dependence of the band edge as

$$E(T) = E(0) - \frac{\alpha_P \cdot \Theta_P}{2}\left[\frac{\rho}{2}\left(\sqrt[4]{1+\frac{\pi^2}{6}\left(\frac{4T}{\Theta_P}\right)^2+\left(\frac{4T}{\Theta_P}\right)^4}-1\right) + (1-\rho)\left(\coth\left(\frac{\Theta_P}{2T}\right)-1\right)\right] \quad (1)$$

with the parameter values listed in Table 1.

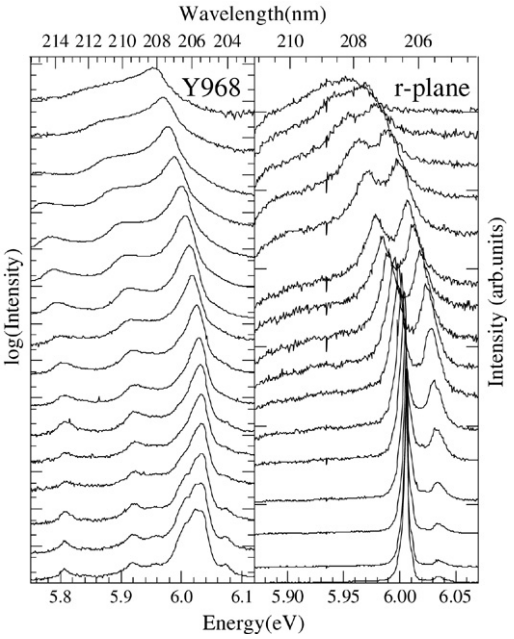

Fig. 3. Left side: CL spectra of sample Y968 at a series of temperatures (8 . . . 300 K) increasing from bottom to top. Right side: PL spectra of the r-plane single crystal.

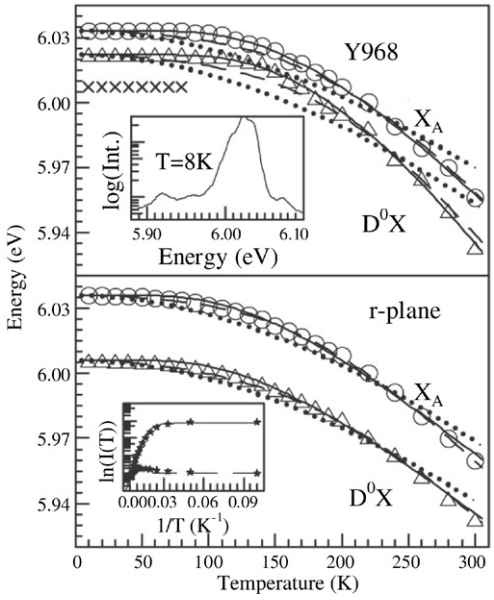

Fig. 4. Upper panel: Energies of two exciton transitions (sample Y968) as a function of temperature. Fits employ the models by Varshni [8, dotted lines], Viña [9, solid lines], and Pässler [10, dashed lines], for parameter values cf. Table 1. The inset shows a CL spectrum of sample Y968 taken at 8 K. Lower panel: Analogous data for the r-plane single crystal. The inset shows an Arrhenius plot of the D^0X (upper curve) and X_A (lower curve) intensities obtained from the temperature dependent PL measurements of the r-plane single crystal. Activation energy of D^0X is $\geq$22 meV.

Table 1
Parameter values for the Varshni, Viña, and Pässler models used to fit the temperature dependent shift of the free and bound exciton lines

	Single crystal		AlN Layer	
	X_A $E(0) = 6.036$ eV	D^0X $E(0) = 6.006$ eV	X_A $E(0) = 6.033$ eV	D^0X $E(0) = 6.022$ eV
Varshni	$\alpha = 0.97$ meV/K $\beta = 1000$ K*	$\alpha = 0.94$ meV/K $\beta = 1000$ K*	$\alpha = 0.91$ meV/K $\beta = 1000$ K*	$\alpha = 0.99$ meV/K $\beta = 1000$ K*
Viña	$B = 0.13$ eV $\Theta = 450$ K	$B = 0.12$ eV $\Theta = 450$ K	$B = 0.2$ eV $\Theta = 560$ K	$B = 0.3$ eV $\Theta = 640$ K
Pässler	$\alpha_P = 0.82$ meV/K $\Theta_P = 730$ K $\rho = 0.25$	$\alpha_P = 0.74$ meV/K $\Theta_P = 680$ K $\rho = 0.23$	$\alpha_P = 1$ meV/K $\Theta_P = 870$ K $\rho = 0.25$*	$\alpha_P = 1.2$ meV/K $\Theta_P = 920$ K $\rho = 0.23$*

Values marked with * were kept constant in the fits.

Temperature dependent PL intensities $I(T)$ were obtained from the r-plane single crystal by fitting the spectra of the donor bound exciton at 6.006 eV and of the X_A free exciton. An Arrhenius plot of the data (Fig. 4 lower inset) yields a thermal exciton activation energy E_{act} for the dominant neutral donor of $\geq$22 meV. This compares quite well with the spectroscopic localisation energy $E_{loc} \approx 30$ meV from the 10 K PL spectra.

3. Conclusions

We have measured reflectance spectra of AlN bulk crystals and MOVPE layers on sapphire at different incidence angles and on different planes. Selection rules allow to assign the X_A and $X_B + X_C$ excitonic band gap energies. Free and bound exciton peaks can be distinguished by temperature dependent CL and PL spectra recorded on the same samples.

Acknowledgement

Partial financial support of this work by the *Deutsche Forschungsgemeinschaft* under contract no. Scho 393/17 is gratefully acknowledged.

References

[1] Y. Taniyasu, M. Kasu, T. Makimoto, Appl. Phys. Lett. 85 (4672) (2004).
[2] K.B. Nam, M.L. Nakarmi, J. Li, J.Y. Lin, H.X. Jiang, Appl. Phys. Lett. 85 (2787) (2003).
[3] L. Chen, B.J. Skromme, R.F. Dalmau, R. Schlesser, Z. Sitar, C. Chen, W. Sun, J. Yang, M.A. Khan, M.L. Nakarmi, J.Y. Lin, H.-X. Jiang, Appl. Phys. Lett. 85 (1) (2004).
[4] E. Silveira, J.A. Freitas Jr., O.J. Glembocki, G.A. Slack, L.J. Schowalter, Phys. Rev. B 71 (041201(R)) (2005).
[5] G.M. Prinz, A. Ladenburger, M. Schirra, M. Feneberg, Y. Taniyasu, M. Kasu, T. Makimoto, R. Sauer, K. Thonke, J. Appl. Phys. (2006) (in press).
[6] B.M. Epelbaum, C. Seitz, A. Magerl, M. Bickermann, A. Winnacker, J. Cryst. Growth 265 (577) (2004).
[7] B.M. Epelbaum, M. Bickermann, A. Winnacker, J. Cryst. Growth 275 (e479) (2005).
[8] Y.P. Varshni, Physica 34 (149) (1967).
[9] L. Viña, S. Logothetidis, M. Cardona, Phys. Rev. B 30 (1979) (1984).
[10] R. Pässler, E. Griebl, H. Riepl, G. Lautner, S. Bauer, H. Preis, W. Gebhardt, B. Buda, D.J. As, D. Schikora, K. Lischka, K. Papagelis, S. Ves, J. Appl. Phys. 86 (4403) (1999).